SUPPORTING APPENDIX for

A stromal region of cytochrome b_6f subunit IV is involved in the activation of the Stt7 kinase in *Chlamydomonas*

Authors: Louis Dumas[1], Francesca Zito[2], Stéphanie Blangy[1], Pascaline Auroy[1], Xenie Johnson[1], Gilles Peltier[1], Jean Alric[1]

Affiliations:
[1]Laboratoire de Bioénergétique et Biotechnologie des Bactéries et Microalgues, CEA, CNRS, Aix-Marseille Université, UMR 7265, BIAM, CEA Cadarache, Saint-Paul-lez-Durance, France
[2]Laboratoire de Biologie Physico-Chimique des Protéines Membranaires, Institut de Biologie Physico-Chimique, CNRS, UMR7099, University Paris Diderot, Sorbonne Paris Cité, PSL Research University, Paris, France, 13 rue Pierre et Marie Curie, F-75005 Paris, France

Text S1. Random mutagenesis by error-prone PCR. Plasmid $pWQH_6$ was used as template in error-prone PCR using kits GeneMorph® II EZClone (Agilent Technologies, "RMA" in Table S1), and Diversify® PCR (Clontech, "RMB" in Table S1). For RMA, 500 ng of pWQH6 plasmid DNA was used as the initial total DNA in a 30 cycles mutagenizing PCR, corresponding to an estimated 25 ng of initial target *petD* DNA, with primers P1-f and P1-r (Table S4) following the PCR conditions detailed in the kit. 400ng of this mutagenizing PCR was used as megaprimer for a second PCR (T_m = 60°C, 25 cycles) to reconstruct the plasmids using Advantage® HD Polymerase mix (Clontech) to facilitate the amplification of AT-rich chloroplast DNA. 1 µl of restriction enzyme *Dpn1* (NEB, 20 U/µL) was added to the PCR reaction to digest methylated (non-mutated) template DNA. XL-10 Gold competent cells were transformed with 4µl of the digestion reaction. ~10% of this transformation mixture was plated on LB-ampicillin (100µg/mL) to control mutagenesis rate by sequencing and the rest was used to inoculate a culture for plasmid amplification and recovery by miniprep (NucleoSpin® Plasmid, Macherey Nagel). For RMB, buffer condition 9 was used in a 25 cycles mutagenizing PCR with 1 ng of $pWQH_6$ and primers P2-f and P2-r (Table S4) following the PCR conditions detailed in the kit. Recovery of $pWQH_6$ plasmids bearing random mutations on *petD* was performed as described for RMA.

Table S1. Random mutagenesis of a region of the *petD* gene by error-prone PCR, amplification of variants in *E. coli* and selection in *C. reinhardtii*.

Mutagenesis trial	*E. coli* transformants				*C. reinhardtii* transformants			
	Total	Sequenced	% Non-mutated	Distribution[c]	Total	Sequenced	% Non-mutated	Distribution[c]
RMA[a]	~250	12	~30%	n.d. (0-6)	~1400	82	~50%	2 (0-3)
RMB[b]	~250	11	0%	n.d. (1-8)	~600	72	~20%	3.5 (0-6)

[a] Mutagenesis using the GeneMorph® II EZClone Domain Mutagenesis Kit (Agilent Technologies).
[b] Mutagenesis using the Diversify® PCR Random Mutagenesis Kit (Clontech).
[c] Peak value of the distribution of mutations along *petD* (number of mutants showing the same number of mutations), with extrema in parentheses. The number of sequenced *E. coli* transformants was too low to give a reliable peak value.

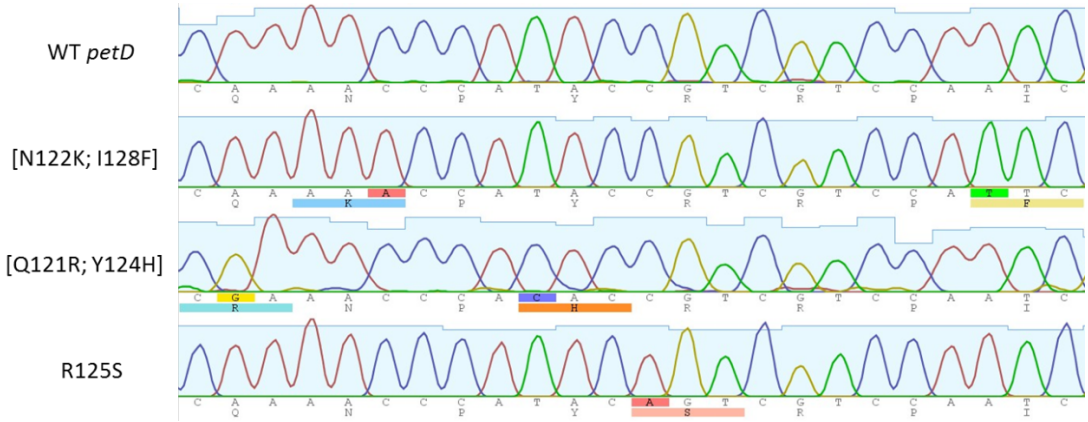

Figure S1. Alignment of the WT *petD* gene (nucleotides 361 to 384) and three *petD* variants obtained by RM. Chromatograms are shown above each sequence. Mutated nucleotides and their corresponding amino-acid substitutions are highlighted in color.

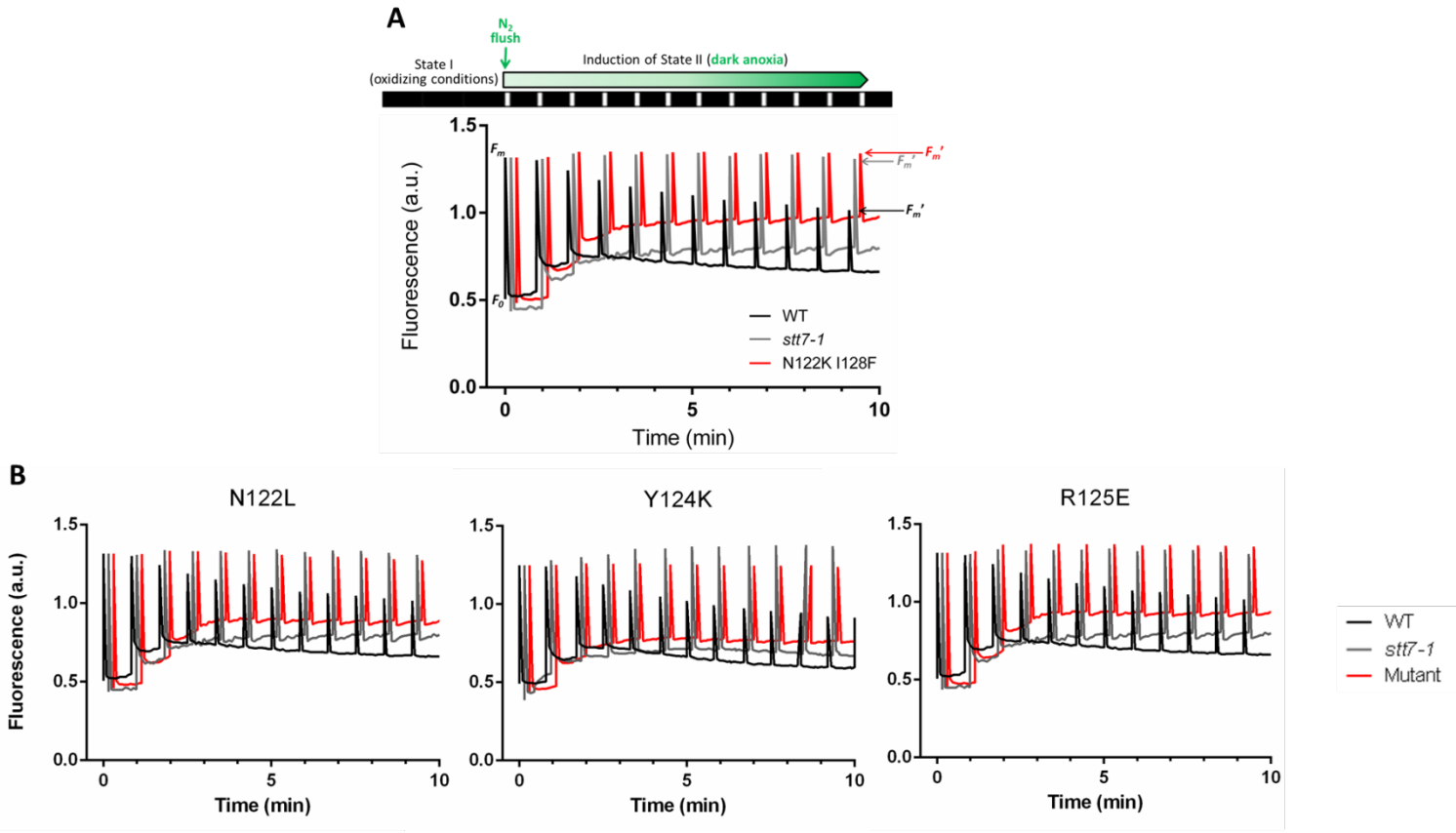

Figure S2. Kinetics of maximum fluorescence yield of PSII upon a transition from dark aerobic to dark anaerobic conditions. One of the *petD* mutant obtained by random mutagenesis (A) and three site-directed *petD* mutants (B) are shown in comparison with the WT and *stt7-1* strains during a 10 min sequence in the dark with 12 saturating flashes giving the maximum fluorescence yield of PSII (F_m). The fluorescence curves were normalized on the value of the maximum fluorescence yield measured after the first saturating flash. The increase of the fluorescence yield in the dark (F'_0) shows that the switch to anaerobic conditions induces the reduction of the PQ pool.

Table S2. List of subunit IV stromal fg loop mutants obtained by random and site-directed mutagenesis of the *petD* gene.

Mutant nb & origin		Helix F	Subunit IV fg loop	Helix G	ST
1	RMA		N118S		++
2	RMB	T110A	N118S	I145T	++
3	SD		N118L		++
4	SD		N118D		++
5	*RMA*	*E74D*	*K119E*		–
6	SD		K119L		++
7	SD		K119E		++
8	RMB		F120S	S154P	+
9	*RMB*	*L95P V104E*	*F120S*	*T130A L132S I145V*	– –
10	*RMB*	*V104A L108H*	*F120L*	*T130S L138F L159S*	– –
11	SD		F120L		++
12	SD		F120W		++
13	*RMB*		*Q121R Y124H*		– –
14	RMB	V104A	Q121R	F149S	++
15	*RMB*	*I117V*	*Q121R N122S*	*L134P F160L*	–
16	SD		Q121L		++
17	SD		Q121R		++
18	*RMA*		*N122I*		– –
19	*RMA*		*N122K*	*I128F*	– –
20	SD		N122T		–
21	SD		N122H		– –
22	SD		N122L		– –
23	RMB		Y124C		++
24	*RMB*		*Y124H*	*F149L*	–
25	RMB		Y124F	I128T T137A L159S	++
26	SD		Y124F		++
27	SD		Y124K		– –
28	*RMA*		*R125S*		–
29	SD		R125L		– –
30	SD		R125E		– –

RM: random mutagenesis; SD: site-directed mutagenesis; ST: state transitions. See Figure S3 for an alignment of the 30 mutants.

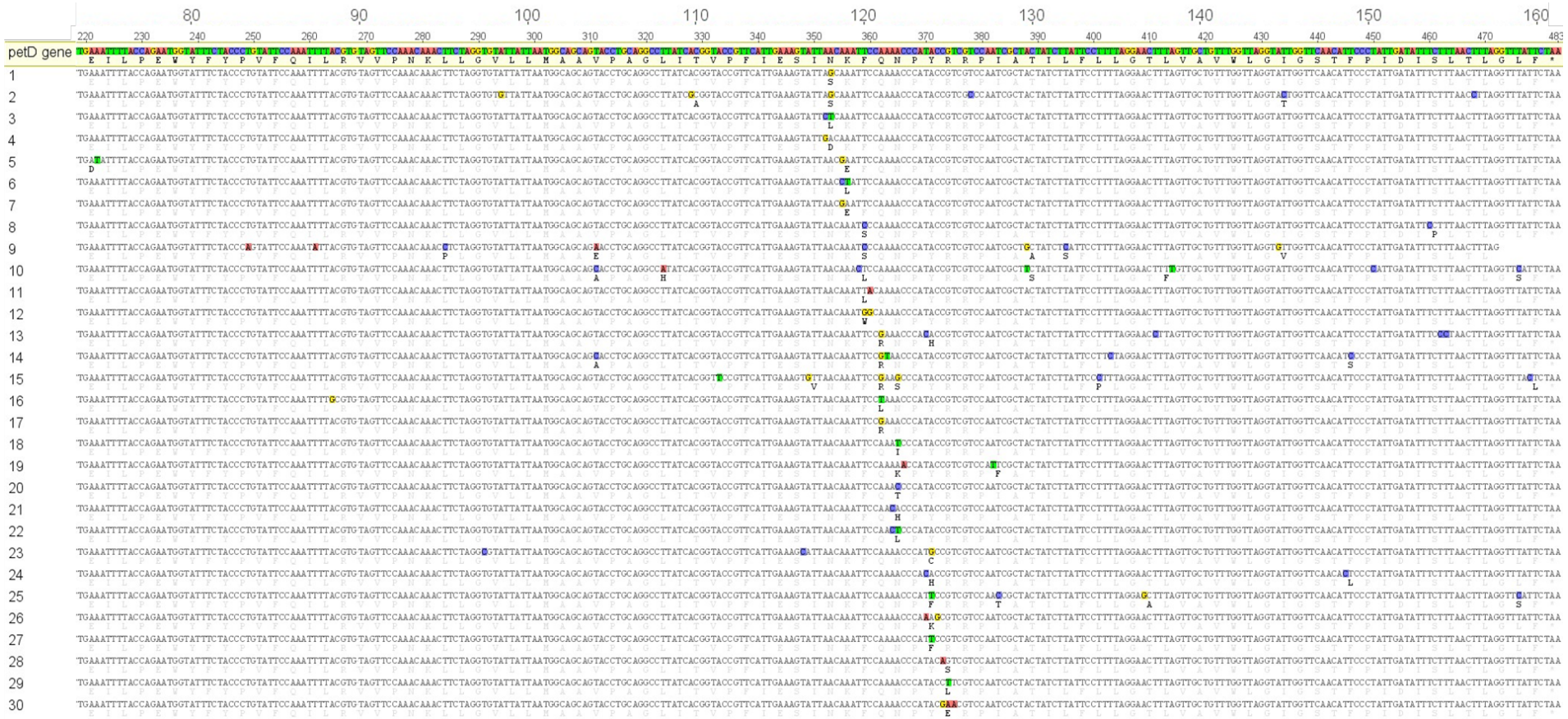

Figure S3. Alignment of nucleotide and amino acid sequences of the 30 random and site-directed mutants of the *petD* gene shown in Table S2 against the WT *petD* sequence. The region of the *petD* sequence shown here (base 219 to terminal base 483) corresponds to the region that was targeted for random-mutagenesis. The amino acid numbering is shown above the nucleotide numbering. Mutated nucleotides are highlighted in color (Red=A, Green=T, Yellow=G, Blue=C). The translated sequences are shown below each corresponding nucleotide sequence using the one-letter amino acid code in grey, except at positions corresponding to non-silent mutations which appear in black.

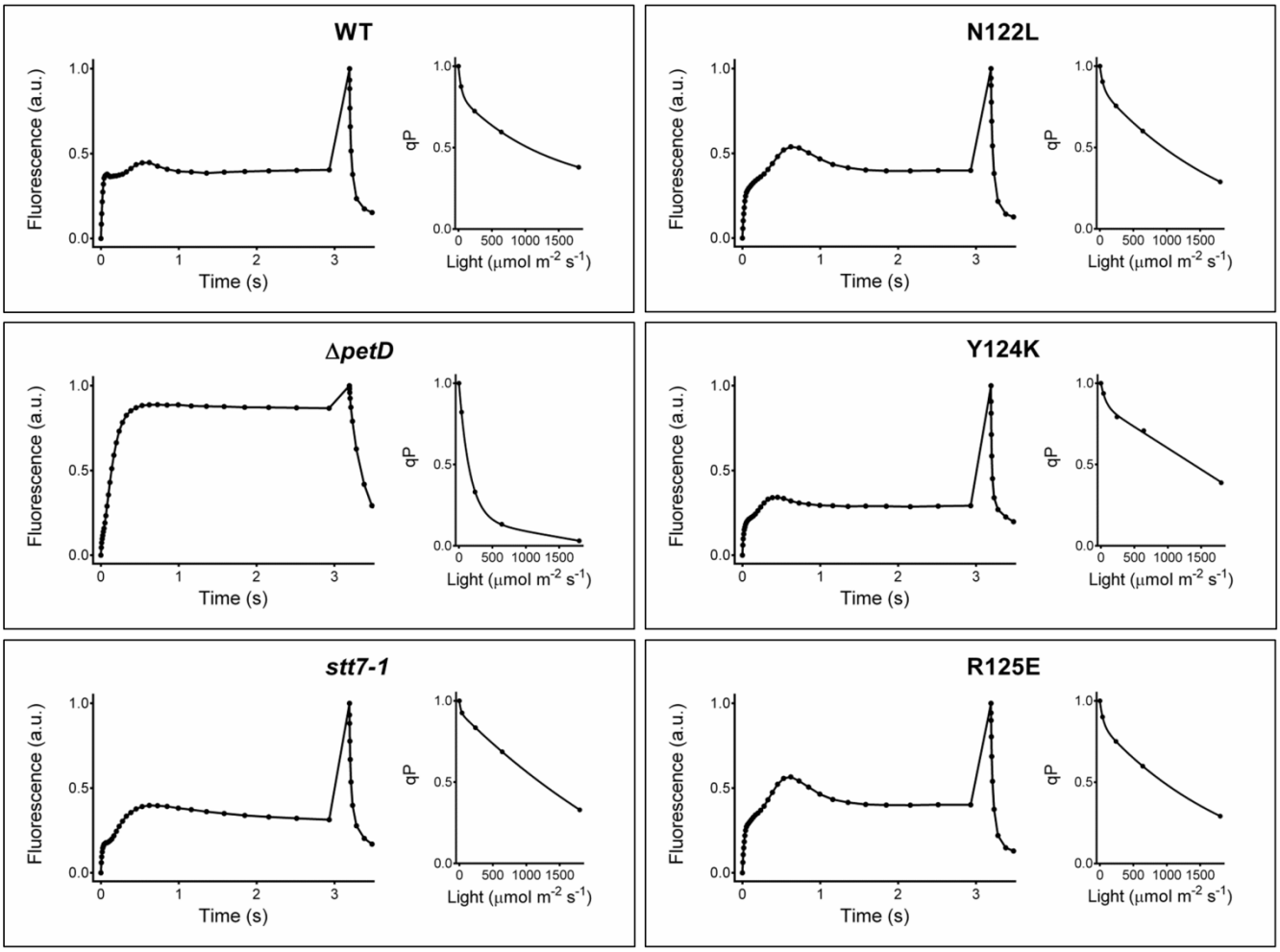

Figure S4. Electron flow through the photosynthetic chain of the three reference and three *petD* mutant strains monitored by chlorophyll fluorescence kinetics normalized between F_0 = 0 and F_m = 1 during a 3 second illumination at 600 µmol photons.m^{-2}.s^{-1}. Photochemical quenching values were calculated ($q_P = (F_m - F)/F_m - F_0$) from fluorescence kinetics at 2s after the onset of illumination and plotted against light intensity.

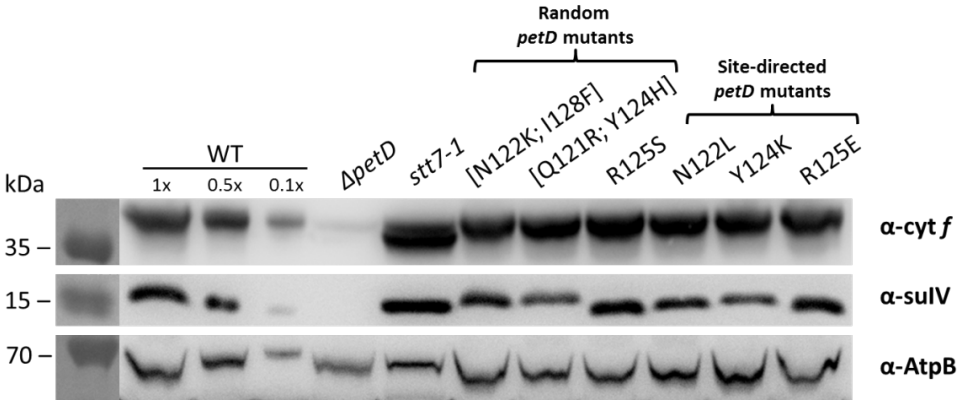

Figure S5. Immunoblots showing the accumulation of cyt *f* and subunit IV in the reference WT (same as Figure 1 of the main text, but including here the 100%, 50% and 10% loading), Δ*petD* and *stt7-1* strains, as well as in three random and three site-directed *petD* mutants. Total proteins were extracted and separated by SDS-PAGE on a 12% gel prior to immunoblotting with specific antibodies. The signal for AtpB was used as a loading control.

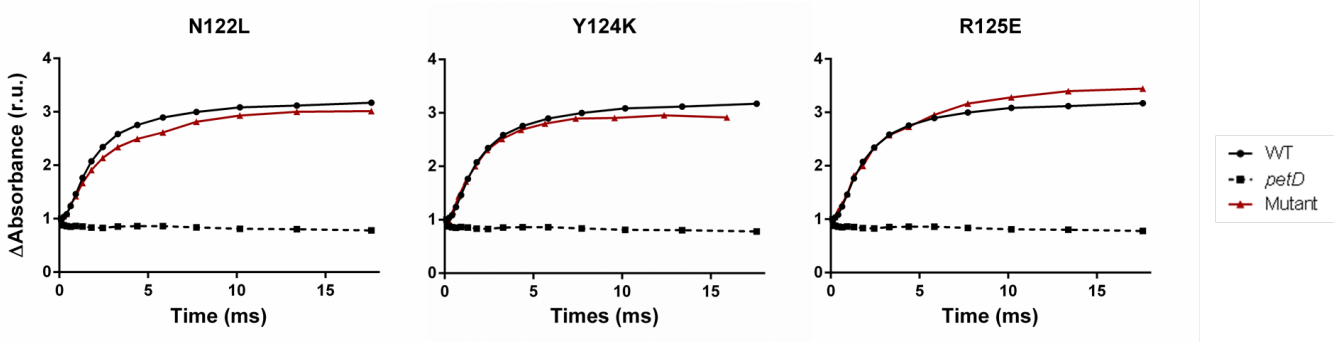

Figure S6. Flash-induced transmembrane electrogenic phase of electron transfer within the cyt b_6f complex. The signal was measured using a Joliot-type spectrophotometer/fluorimeter (JTS-10, Bio-Logic) as the electrochromic shift (ECS) of carotenoids giving an absorbance increase at 520 nm (1). Electron transfer reactions were measured under anaerobic conditions following a single-turnover of PSI (10 ns flash, 10 mM hydroxylamine and 10 µM DCMU added to inhibit PSII) and normalized on PSI contribution at 100 µs (hence the relative units of the vertical axis).

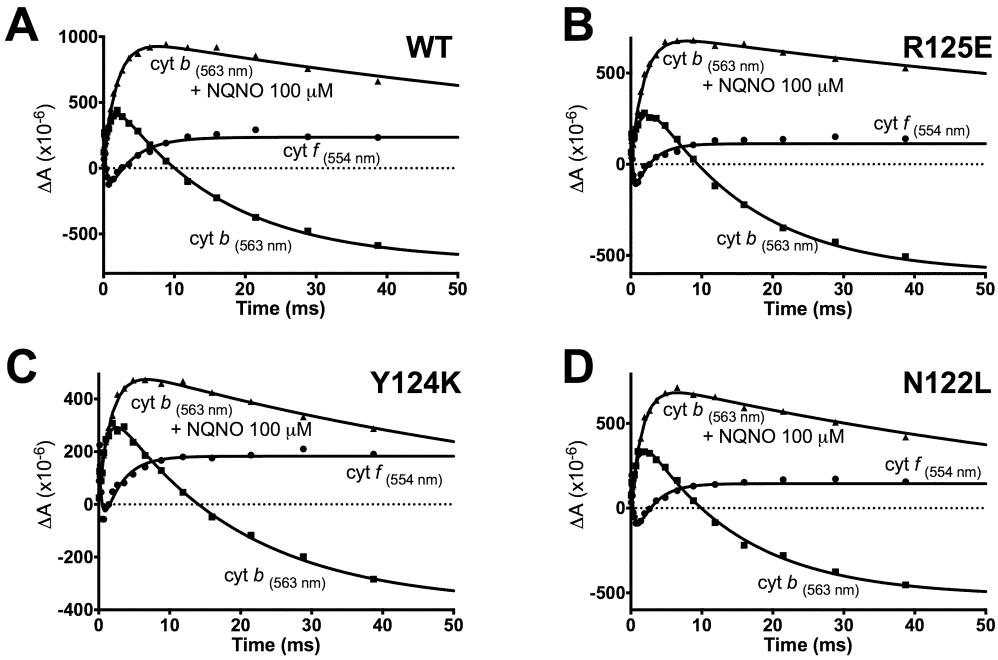

Figure S7. Kinetics of absorbance changes following a single turnover of PSI (PSII was inhibited by 1 mM hydroxylamine and 10 µM DCMU, excitation is a very short laser flash of 10 ns) obtained in whole cells suspensions adapted under dark-anaerobic conditions (conditions similar to Figure S6 above). Kinetics were obtained for the control strain and the three site-directed mutants R125E, Y124K and N122L at two different detecting wavelengths, 554 nm for cytochrome *f*, and 563 nm for the *b*-hemes. An absorbance increase corresponds to reduction, a decrease to oxidation (1). Cyt *f* is oxidized (by plastocyanin) in about ~300 µs and reduced (by Q_o) in ~5 ms. Heme b_H is pre-reduced in the dark-anaerobic state. Absorbance increase at 563 nm (~5 ms) therefore represents heme b_L reduction. Whereas it is very stable (> 100 ms) when the Q_i site is inhibited with NQNO, it is only transient in its absence (~15 ms), and the oxidation of b_L and b_H is observed at > 30 ms after the flash, showing equally fast electron transfer to the quinone at the Q_i site.

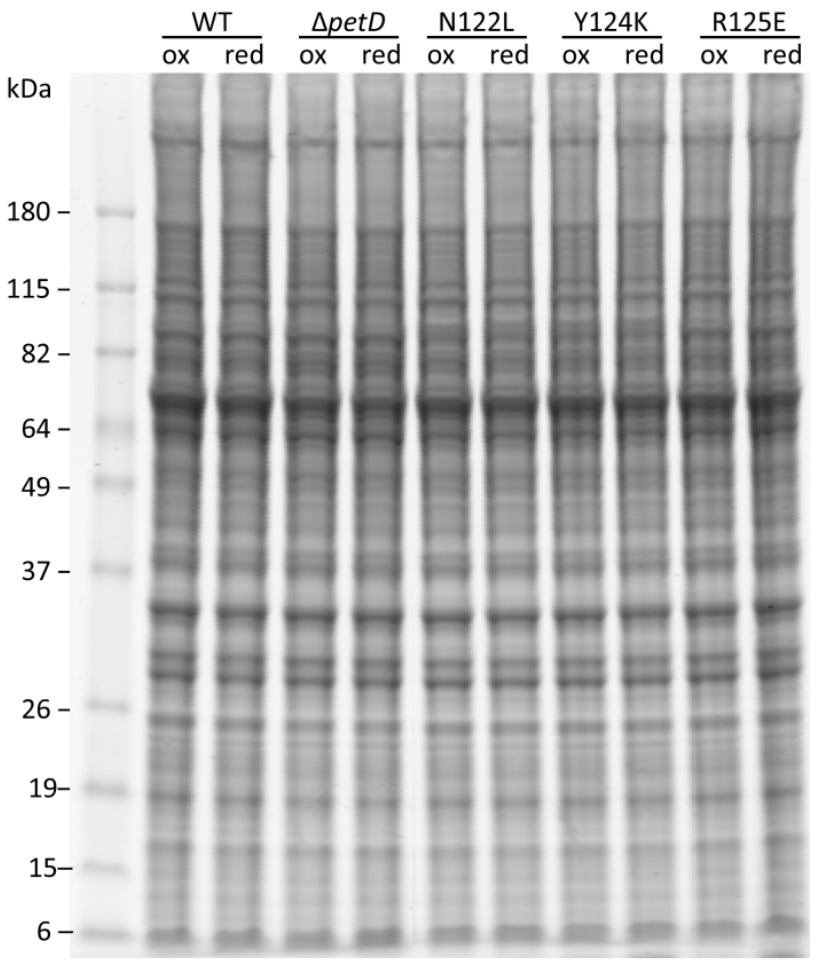

Figure S8. Coomassie blue staining of a 10% Bis-Tris gel loaded with total cell extracts from the Δ*petD* and WT strains in comparison to the three SD *petD* mutants, normalized on chlorophyll content.

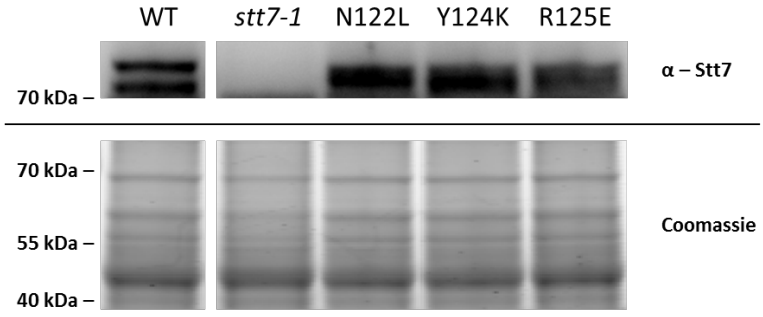

Figure S9. Western-Blot analysis of Stt7 accumulation in complemented lines (top panel) with Coomassie-blue staining as a loading control (bottom panel). The expected molecular weight of Stt7 is 80 kDa. Stt7 antibody was a kind gift of Michel Goldschmidt-Clermont (University of Geneva). Stt7 is recognized as a smeary doublet band (absent from the *stt7*-1 deletion strain), similarly as in Figures S1-3 of (2). Stt7 accumulation is not affected in the *petD* mutant strains.

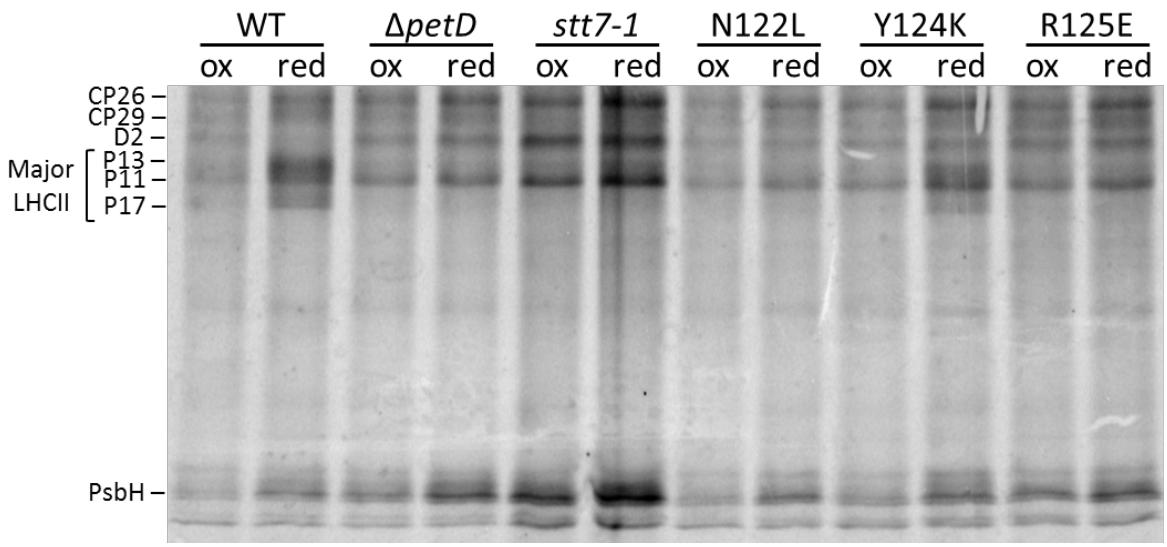

Figure S10. Autoradiogram of *in vivo* ^{33}P-labeled polypeptides in reducing conditions. Thylakoid proteins were extracted from cells placed in State 1 (10 µM DCMU, moderate light, strong agitation, 30 min) or State 2 (2 mg/ml glucose oxidase, 20 mM glucose, dark, 30 min) conditions and separated by SDS-PAGE on a 8 M urea 12-18% gradient gel.

Text S2. Yeast two-hybrid assays. The Matchmaker® Gold Yeast Two-Hybrid System (Clontech) was used to test the direct interaction between subunit IV and Stt7. The nucleotide sequences of the WT and [Y124K; R125E] mutant subunit IV fg loops were cloned as baits into pGBKT7 vectors and various Stt7 nucleotide sequences were cloned as preys into pGADT7 vectors. All vector constructions were verified by sequencing. Y2H Gold yeast cells were transformed with each pGBKT7-suIV vector and Y187 yeast cells were transformed with each pGADT7-Stt7 vector following the small-scale LiAc yeast transformation procedure described in the Yeast Protocols Handbook (Clontech). None of the strains transformed with pGBKT7-suIV plasmids exhibited autoactivation of the reporter genes when spotted on medium lacking Trp and containing 40 µg.ml^{-1} X-α-Gal and 150 ng.ml^{-1} Aureobasidin A. Diploids containing each bait-prey plasmid combination (Figure S11) were obtained following the yeast mating protocol described in the Handbook and conserved on medium lacking Leu and Trp. Positives clones were selected on medium lacking Trp, Leu and His, supplemented with 40 µg.ml^{-1} X-α-Gal with or without 150 ng.ml^{-1} Aureobasidin A. The positive and negative controls were obtained as described in the Matchmaker® Gold User Manual (Clontech).

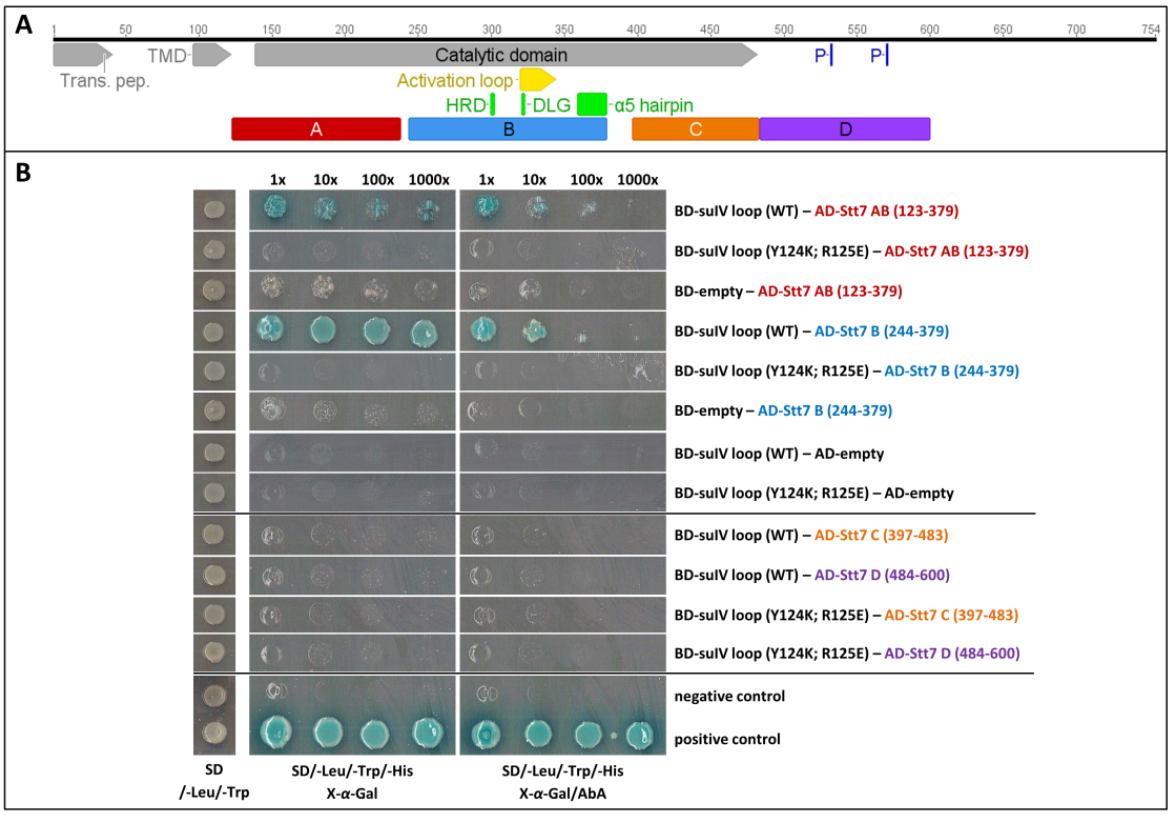

Figure S11. Yeast two-hybrid assay of the interaction between cyt b_6f subunit IV and Stt7 kinase domain. (A) Schematic diagram of the full annotated Stt7 protein sequence. Trans. pep. = transit peptide; TMD = transmembrane domain; P = previously identified phosphorylation sites (3, 4). The activation loop is annotated in yellow and the catalytic motifs HRD and DLG as well as the α5-hairpin region (5) are colored in green. (B) Images of yeast cells spotted on various media. Double drop-out medium (SD/-Leu/-Trp) is used to select for diploids following yeast mating. Triple drop-out media (SD/-Leu/-Trp/-His) supplemented with 40 µg.ml^{-1} X-α-Gal with or without 150 ng.ml^{-1} Aureobasidin A (AbA) are used to select positive clones containing interacting peptides.

Text S3. Cloning, expression and purification of Stt7-KD. The full-length *stt7* gene (*C. reinhardtii* accession no. Q84V18) was recoded for *E. coli* codon bias and synthesized (Invitrogen). The 1.0 kb nucleotide sequence coding for the catalytic domain of Stt7 (residues 139 to 495) with an added C-terminal Strep-tag was cloned with the InFusion® HD Cloning Kit (Clontech) into expression vector pLIC03 under the *LacZ*-inducible operon. The resulting plasmid was used to transform *E. coli* BL21DE3 Rosetta cells for overexpression. Cultures of *E. coli* BL21DE3 Rosetta cells were grown at 37°C, induced at an optical density of 0.6-0.8 with 400 µM IPTG and grown overnight at 17°C. Cells were harvested by centrifugation (4000 *g*, 20 min, 4°C), resuspended in lysis buffer (50 mM Tris Buffer, 300 mM NaCl, 2.5 mM *β*ME, 0.25 mg.ml^{-1} lysozyme, 5% glycerol, protease inhibitor cocktail (pH 8.0)) and frozen at -80°C. The thawed cells were then lyzed by sonication and centrifuged (15000 *g*, 40 min, 4°C). Stt7-KD was then purified on an ÄKTA-Pure chromatography system. The clear supernatant was loaded on a hand-packed column containing Streptavidin Sepharose™ HP beads (5 ml, GE) pre-equilibrated with Buffer A (50 mM Tris Buffer, 300 mM NaCl, 2.5 mM *β*ME (pH 8.0)). Unbound or weakly bound proteins were washed with Buffer A and bound proteins eluted with Buffer A supplemented with 2.5 mM desthiobiotin (Figure S12 Panel A). The elution fractions were pooled and loaded on a HisPur™ Ni-NTA column (1 ml, ThermoFisher) pre-equilibrated with Buffer B (50 mM Tris Buffer, 300 mM NaCl, 2.5 mM *β*ME, 10 mM imidazole (pH 8.0)). Unbound or weakly bound proteins were washed with Buffer B. The column was washed with Buffer B containing 34 mM imidazole and His-tagged Stt7-KD was eluted with Buffer B containing 250 mM imidazole (Figure S12 Panel B). The pooled elution fractions were transferred to a new buffer (20 mM HEPES-KOH, 300 mM NaCl, 2.5 mM TCEP (pH 8.0)) and concentrated for subsequent *in vitro* experiments. Figure S12 Panel C shows SDS-PAGE analysis of the purification procedure.

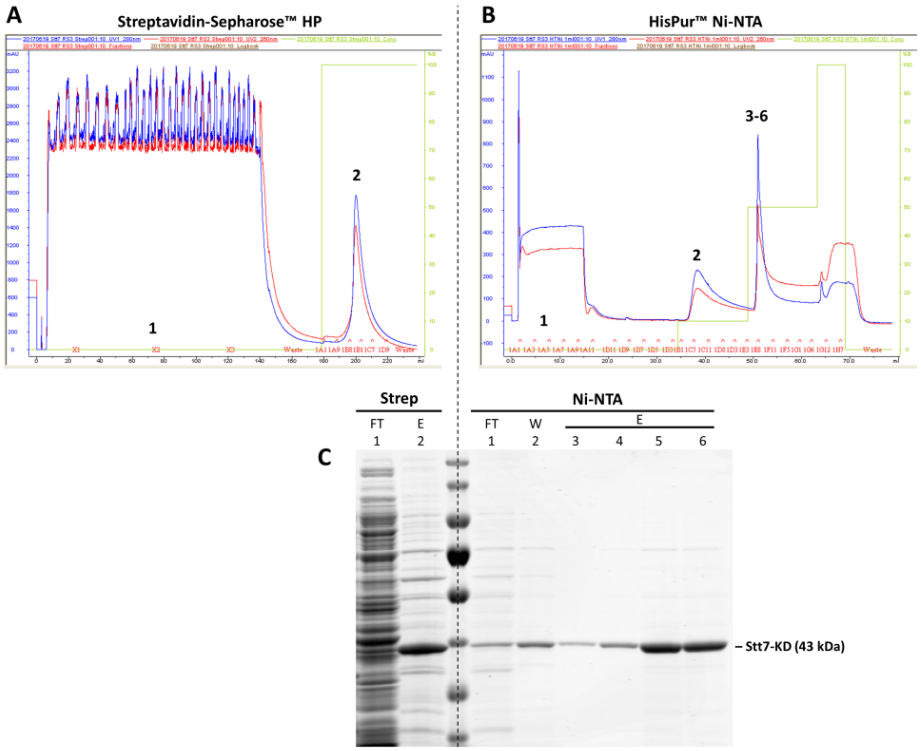

Figure S12. Purification of Stt7 kinase domain. Absorbance chromatograms showing the elution profiles of the Streptavidin Sepharose™ HP column (A) and the HisPur™ Ni-NTA column (B). Wash or elution steps are depicted by the green curves. Representative elution fractions were analyzed by SDS-PAGE (C). FT: flow-through; W: wash; E: elution.

Table S3. Stt7 kinase domain shows ATP hydrolysis activity. Following the protocol of the ADP-Glo™ Kinase Assay kit (Promega), 1 µM purified Stt7-KD was incubated with 1 mM ATP in a 25 µl kinase reaction containing 40 mM Tris-HCl, 20 mM $MgCl_2$ and 0.1 mg/ml BSA at room temperature for 30 minutes. An equal volume of ADP-Glo™ Reagent was added to the reaction and left to incubate at room temperature for 40 min to deplete the residual unconsumed ATP. 50 µl of Kinase Detection Reagent containing luciferase and luciferin was then added to convert ADP to ATP and generate a stable luminescence signal, proportional to the amount of ADP produced during the kinase reaction and therefore correlated with Stt7-KD activity. After incubation at room temperature for one hour, the luminescence signal was measured on an Infinite M200 luminometer (TECAN). The luminescence value for the control experiment (same conditions with no Stt7-KD added) was subtracted from the luminescence values of the two experiments shown here. For these, three independent kinase reactions were carried out for the calculation of mean values and standards deviations.

	1 µM Stt7-KD 1 mM ATP	**2 µM Stt7-KD 1 mM ATP**
Luminescence (a.u.)	7,55 ± 0,63	11,62 ± 0,50

Figure S13. Alignment of subunit IV from various organisms pertaining to the green lineage with cytochrome *b* polypeptides from cytochrome bc_1 complexes. The subunit IV fg loop motif NKFQNPxRR is conserved through the green lineage but shows a strong divergence with cytochromes *b*.

Table S4. Oligonucleotides used for random and site-directed mutagenesis of the *petD* gene using plasmid pWQH$_6$.

Name	5'-start on pWQH6 plasmid	Sequence	Use
P1-f	4109	ACCCATTTGCTACTCCACTTG	*petD* random mutagenesis A (RMA) primers
P1-r	4465	TGACAGAACTCAGTTTTCCCC	
P2-f	4109	TGGGTGAGCCAGCAAACCCATTTGCTACTCCACTTG	*petD* random mutagenesis B (RMB) primers
P2-r	4465	TGACAGAACTCAGTTTTCCCCCTTCAGGGTTGC	
N122L-f	4255	AGTATTAACAAATTCCAA**CT**CCCATACCGTCGTCCAATC	*petD* site-directed mutagenesis primers
N122L-r	4294	GATTGGACGACGGTATGGG**AG**TTGGAATTTGTTAATACT	
Y124K-f	4261	AACAAATTCCAAAACCCA**A**A**G**CGTCGTCCAATCGCTACT	
Y124K-r	4300	AGTAGCGATTGGACGACG**C**T**T**TGGGTTTTGGAATTTGTT	
R125E-f	4264	AAATTCCAAAACCCATAC**GAA**CGTCCAATCGCTACTATC	
R125E-r	4303	GATAGTAGCGATTGGACG**TTC**GTATGGGTTTTGGAATTT	

References

1. Joliot P & Joliot A (1998) In vivo analysis of the effect of dicyclohexylcarbodiimide on electron and proton transfers in cytochrome bf complex of Chlorella sorokiniana. *Biochemistry* 37(29):10404-10410.
2. Lemeille S*, et al.* (2009) Analysis of the chloroplast protein kinase Stt7 during state transitions. *PLoS biology* 7(3):e45.
3. Bergner SV*, et al.* (2015) STATE TRANSITION7-Dependent Phosphorylation Is Modulated by Changing Environmental Conditions, and Its Absence Triggers Remodeling of Photosynthetic Protein Complexes. *Plant physiology* 168(2):615-634.
4. Lemeille S, Turkina MV, Vener AV, & Rochaix JD (2010) Stt7-dependent phosphorylation during state transitions in the green alga Chlamydomonas reinhardtii. *Mol Cell Proteomics* 9(6):1281-1295.
5. Guo J*, et al.* (2013) Structure of the catalytic domain of a state transition kinase homolog from Micromonas algae. *Protein & cell* 4(8):607-619.